PAPER • OPEN ACCESS

Comparative studies of GelMA hydrogels: investigating the effect of different source on mechanical, physical and biological properties

To cite this article: Hilal Yilmaz *et al* 2024 *Mater. Res. Express* **11** 075307

Materials Research Express

PAPER

Comparative studies of GelMA hydrogels: investigating the effect of different source on mechanical, physical and biological properties

Hilal Yilmaz[1,2,3], **Sevda Gursoy**[1,2,3], **Hilal Calik**[3], **Yagmur Kazancioglu**[3], **Ridvan Yildirim**[1], **Rabia Cakir**[3], **Oguzhan Gunduz**[1,2,4], **Arsalan Ahmed**[5] and **Cem Bulent Ustundag**[1,2,3]

[1] Center for Nanotechnology & Biomaterials Application and Research (NBUAM), Marmara University, Istanbul, Turkey
[2] Health Biotechnology Center for Excellence Joint Practice and Research, (SABIOTEK), Yildiz Technical University, Istanbul, Turkey
[3] Department of Bioengineering, Faculty of Chemical and Metallurgical Engineering, Yildiz Technical University, Istanbul, Turkey
[4] Department of Metallurgical and Materials Engineering, Faculty of Technology, Marmara University, Istanbul, Turkey
[5] Interdisciplinary Research Centre in Biomedical Materials, COMSATS University Islamabad, Lahore, Pakistan

E-mail: hilaltoptas44@gmail.com

Keywords: gelatine, GelMA hydrogel, PVP nanoparticle, tissue engineering

OPEN ACCESS

RECEIVED
7 May 2024

REVISED
30 June 2024

ACCEPTED FOR PUBLICATION
12 July 2024

PUBLISHED
24 July 2024

Abstract

GelMA hydrogels are prominent in biomedical applications due to their innate extracellular matrix mimicking properties. They exhibit favorable properties for cell proliferation and formation of light-induced hydrophilic cross-linked structures. However, there is limited research on the effect of variations in the starting material (gelatin) on the physical, mechanical and biological properties. In this study, Gelatin Methacrylic Anhydride (GelMA) hydrogels were synthesized from two different products of type B gelatin and loaded with polyvinylpyrrolidone (PVP) nanoparticles by electrospray method. Chemical and structural analyses were performed by FTIR, ^{1}HNMR, TNBS and SEM, respectively. Mechanical properties were evaluated by compression tests. Cytocompatibility was evaluated by XTT analysis. GelMA hydrogels obtained from two brands have suitable pore size, mechanical strength, swelling properties and cytocompatibility, making them suitable for various biomedical applications. In addition, the addition of PVP nanoparticles can make them useful for drug delivery applications.

1. Introduction

Hydrogels developed from biocompatible gelatin formed by partial hydrolysis of collagen, the most abundant protein in living organisms, have recently become very popular [1]. It has many applications in medical/pharmaceutical, technical, food and cosmetic products. One of the important features of gelatin, which has good solubility and low antigenicity compared to collagen, is that it has very specific structures that enable cell adhesion and remodeling, such as arginine-glycine-aspartic acid (RGD) sequences and matrix metalloproteinase (MMP) target sequences [1–3]. To overcome the disadvantages of gelatin hydrogels, such as lack of stability at body temperature, rapid degradation, and low mechanical modulus, they are subjected to various chemical modifications by utilizing -OH, -COOH, -NH_2, -SH, and similar active groups in their side chains [4]. Among them, GelMA, which is prepared in different application forms to meet different application needs, is the most popular [3, 4]. GelMA has been used in many applications and forms since it was first synthesized in 2000 from the reaction of gelatin with methacrylic anhydride [5]. This synthesis occurs through the exchange of amino groups and methacryloyl groups. GelMA hydrogels, which gain the ability to photocrosslink under UV light when photoinitiator is added due to the presence of methacryloyl groups in its structure, retain the presence of MMP and RGD sequences, which are the main advantages of gelatin, biocompatibility and biodegradability. In addition, unlike gelatin, it has the advantage of maintaining its stability and shape at body temperature [2, 6]. Biocompatible GelMA hydrogels contribute to tissue repair by providing an ECM environment for cells. Photopolymerization is a widely used method for producing protein-based hydrogels such as GelMA. It allows proteins to be easily prepared and mechanically modified without losing

their natural bioactivity. In this context, GelMA is one of the most remarkable protein-based biomaterials produced through photopolymerization [7]. Gelatin, a versatile biopolymer, is commonly produced from bovine, poultry and fish. Due to differences in production sources, there are differences in chemical composition (molecular weight, amino acid content and isoelectric points) and structure-function. Bovine and porcine gelatins are most commonly used for GelMA synthesis [8]. Therefore, GelMA can be divided into two types according to whether they are derived from type A or type B gelatin. Gelatin derived from porcine skin is commonly known as type A gelatin and is reported to have more free carboxyl groups and a higher isoelectric point compared to type B gelatin derived from bovine skin. There is also great interest in the development of efficient methods to produce GelMA with high reproducibility and controllability in terms of composition and biophysiochemical properties for sustainable GelMA production in the food industry and pharmacology [9].

The most important criterion in these studies is to systematically ensure the reproducibility and controllability of the synthesis. A common feature of GelMAs is that the physical properties of the hydrogels vary depending on the degree of methacrylation, initial gelatin concentration (w/v), photoinitiator concentration (w/v) and light exposure time [10]. The brand supplied and even the batches within brands are as important as the initial gelatin concentration. In this context, studies have generally proceeded with the synthesis of GelMA from commercially available gelatin from Sigma-Aldrich [10–12].

The photocrosslinking, controlled degradation and mechanical properties of GelMA hydrogels may facilitate [1, 3, 4] their combination with bioactive components, cytokines, exosomes, cells, nanoparticles and drugs. This may make it attractive for many biomedical applications [7, 13–16]. Wang *et al* compared GelMAs prepared from gelatins of different origins with the commonly used porcine gelatin. GelMAs produced from gelatins of different origins, which overcome the thermal gelation problem of porcine gelatin, were compared chemically, mechanically, physically, and biologically. As a result, they reported that GelMAs prepared from cold-soluble gelatin are promising for the development of bioinks [17]. Gaglio *et al* In his study, he focused on the chemical, physical, mechanical, and biological effects of degree of functionalization (DoF) modulation on the properties of GelMAs synthesized from both type A and type B by different methods, drawing attention to the DoF of GelMAs. In addition, their efficiency as bioinks in 3D printing was also investigated. When the synthesis protocols of GelMAs produced from type A gelatin were compared with those obtained from type B gelatin, their performances showed significant differences, indicating the need for further studies in this area. It has also been reported that GelMAs produced from type B gelatin have a more sustained potential on cell viability than GelMAs produced from type A gelatin [18]. Our goal is not to replace Sigma gelatin with Halvet gelatin, but to show that Halvet gelatin has similar physical, chemical, mechanical and biological properties to Sigma gelatin, demonstrating its potential for biomedical applications. In addition, it was observed that GelMA obtained from Halvet gelatin exhibits similar physical, chemical, mechanical and biological properties to GelMA obtained from Sigma gelatin, and it is predicted that it has potential for biomedical applications.

Processes to produce smaller particles in drug delivery systems include ionic gelation, high temperature treatments, homogenization, electrospray (ES), and spray drying [19]. Electrohydrodynamic atomization (EHDA), also known as ES, is a simple way to produce particles of desired size through single or multi-step processes [20]. In the last two decades, MP/NPs produced by ES using polymeric materials have become of interest for biomedical applications [12]. In this technique, electrostatic forces are used to form nano- to macro-sized fibers or particles by manipulating an electrically charged liquid jet. Through various methods such as mixing, surface modification and coaxial processes, it is possible to integrate bioactive molecules such as drugs, proteins, cells, DNA and growth factors into carriers produced by EHDA techniques [21].

Polymeric micro/nanoparticles (MP/NP) made of biodegradable polymer can provide sustained and controlled release compared to conventional drug delivery vehicles, protect drugs from chemical and enzymatic degradation, prolong their *in vivo* half-life, and improve cell membrane and blood–brain barrier penetration. They can overcome physiological barriers and can also be targeted to cells, tissues, or organs with more efficient delivery or reduced side effects [22]. Polyvinylpyrrolidone (PVP) is one of the most widely used FDA-approved polymers in the pharmaceutical, medical, and cosmetic fields [23]. PVP is a water-soluble, biodegradable, non-toxic, and biocompatible polymer. It has C=O, C-N and CH_2 functional groups, which are widely used in NP synthesis. In addition, it contains a strong hydrophilic component (pyrrolidone moiety) and a significant hydrophobic group (alkyl group), which give it amphiphilic properties [24]. It can be encapsulated with drugs or bioactive ingredients [25]. Edikresnka *et al* successfully synthesized PVP composite nanostructures loaded with green tea extract (GTE) as an active ingredient using ES technique and showed from SEM images that PVP/GTE nanostructures have a combination of less spherical particles and nanofibers [26].Chhouk *et al* To increase the bioavailability of a small amount of water-soluble curcumin, they reported that they increased the dissolution of curcumin/PVP particles in water by preparing curcumin-containing PVP microspheres by electrospraying [27]. Rezeki *et al* reported that they successfully prepared PVP/mangosteen pericarp extract (MPE) particles [28]. Guastaferro *et al* successfully produced microparticles and microfibers of quercetin (QT)-loaded PVP via an electrohydrodynamic process supported by supercritical CO_2 [29]. Ali *et al* reported their studies on drug release

by coating metal microneedles with the ES method using PVP [30]. Belyy *et al* reported that it forms a strong complex with the lignin-PVP complex and contributes to the stability of the lignin colloidal solution through steric stabilization [31]. Xu *et al* developed core–shell nanoparticles using the ES method. They developed a modified coaxial ES method for drug preparation based on the use of PVP cellulose acetate (CA) in the shell portion as an acetaminophen (ATP)-based sustained release carrier [32]. To our knowledge, our study is the first to report the application of PVP particles to GelMA hydrogels using the ES method.

The aim of this study was to synthesize GelMA from Sigma gelatin, which is widely used in the literature, and Halvet gelatin, which may be its equivalent, and to compare their chemical, morphological, physical and biological behavior. It was found that even the batch number of the gelatin used in the synthesis of GelMA had an effect on the properties of GelMA hydrogells, while two different brands had similar properties. GelMA synthesized from both products was then coated with PVP particles, a candidate drug/biological carrier, using the electrospray method. To the best of our knowledge, this study is the first example in the literature where GelMAs from different type B gelatins were compared and coated with PVP particles. We report relatively favorable swelling performance, good mechanical properties, and cytocompatibility for use in biomedical applications. We find that the Halvet GelMA hydrogels obtained in the study exhibit similar physical, chemical, mechanical, and biological properties to Sigma GelMA hydrogels. We envision that both GelMA hydrogels can be coated with PVP and evaluated for their chemical, mechanical and physical properties to find a place in any application where tissue engineering and drug delivery systems are co-designed.

2. Materials and methods

2.1. Materials

Gelatin type B from bovine skin was bought from Halvet (Turkey) and Sigma Aldrich (Germany). Sigma-Aldrich/G9391 Gelatin (Type B, gel strength~225 g Bloom) and Halvet/0797-21 (Type B, gel strength~gel 230–250 g Bloom). Methacrylic anhydride (MAA) (276685–100 ml), 2-Hydroxy-4'-(2-hydroxyethoxy)-2-methylpropiophenone (ırgacure) (410896–10 G), Polyvinylpyrrolidone (PVP): molecular weight 40,000 Da, TNBS solution (5% (w/v) in water), sodium dodecyl sulfate (SDS), ethanol (C_2H_5OH) and dialysis membrane (cut-off value 14 kDa and average flat width 43 mm) were obtained from Sigma Aldrich (Germany). Sodium carbonate, sodium hydroxide, hydrochloric acid fuming 37% were purchased from Merck (Germany). Phosphate-buffered saline (PBS, pH 7.4) was bought from ChemBio (Turkey). Sodium hydrogen carbonate (>99.7%) was purchased from ISOLAB (Germany).

2.2. Methods

2.2.1. GelMA synthesis and preparation of hydrogels

A previously established protocol was followed to synthesize GelMA from the type B gelatins used in the study [33]. The reason for using 0.2 ml of MAA per gram is that type B gelatin contains more amine groups than type A [34]. Briefly, a 10% (w/v) gelatin solution was allowed to dissolve in 0.1 M bicarbonate buffer at 60 °C. Then, 0.2 ml of methacrylic anhydride (MAA) per gram of gelatin was added to the gelatin solution and allowed to react at 50 °C for 3 h with constant stirring. To remove unreacted MAA and methacrylic acid by-products, the resulting solution was dialyzed in distilled water at 40 °C for 3 days. It was then lyophilized for three days and stored at −20 °C until use. The hydrogel was prepared by covalent crosslinking in a UV curing apparatus using 20% GelMA and 5 mg irgacure per ml in approximately 7 min. It was named GelMA1, synthesized from gelatin (Sigma), and GelMA2, synthesized from gelatin (Halvet).

2.2.2. Preparation of solutions for electrospray

A 10% w/v PVP solution was used in the study. The solution was prepared in a magnetic stirrer at 200 rpm until dissolved in ethanol. PVP particles were prepared by the electrospray method in a Basic system (Inovenso, Istanbul, Turkey) [35]. The distance between the collector and the needle was set at 12.5 cm and a voltage of 18 kV was applied at a flow rate of 0.8 ml/h. To collect PVP particles, a glass coverslip and then GelMA1 and GelMA2 hydrogels were placed on the collector dried appropriately, and stored for characterization.

2.2.3. Characterization of particle-loaded hydrogels

2.2.3.1. Chemical structure analysis

Fourier transform infrared spectroscopy (FTIR, FT/IR-ATR 4700, Jasco, Easton, MD, USA) was used to determine the chemical structure of PVP, Gelatin Sigma, Gelatin Halvet, GelMA (Sigma), GelMA (Halvet), GelMA (Sigma) @PVP and GelMA (Halvet) @PVP. Measurements were performed at room temperature with a resolution of 4 cm^{-1} in the wavelength range 450–4000 cm^{-1}.

The degree of substitution (DS) of GelMA was investigated using ^{1}H NMR spectroscopy (Bruker Avance Neo 500 MHz, Bremen, Germany). Both gelatin and GelMA were dissolved at a 10 mg ml^{-1} concentration in D_2O; ^{1}H-NMR spectra were obtained at a frequency of 500 MHz and room temperature. The DS of GelMA was calculated according to the following equation (1):

$$DS(\%) = 1 - \frac{(peak\ area\ of\ GelMA\ lysine\ methtlene)}{(peak\ area\ of\ gelatin\ lysine\ methtlene)} \times 100\% \quad (1)$$

The DS value of GelMA was also determined by the TNBS method [11, 36]. GelMA and gelatin samples were dissolved in 0.1 M sodium bicarbonate (pH 8.5) buffer to a concentration of 0.5 mg ml^{-1}. 250 μl of 0.01% TNBS solution were added to 500 μl of each sample, and the mixture was incubated in the dark at 40 °C for 2 h. To stop the reaction, 250 μl of 10% (w/v) SDS and 125 μl of 1 M hydrochloric acid solutions were added. The UV absorbance of each sample was measured at 335 nm (UV-1280, Shimadzu, Japan). Glycine standard solutions with concentrations of 0, 1, 5, and 10 μg ml^{-1} were used to determine the amino group concentration.

2.2.3.2. Morphology of hydrogels

The surface morphology of GelMA1, GelMA2, and PVP particules were examined using a scanning electron microscope (SEM) (EVA MA 10, Zeiss, Jena, Germany). GelMA1 and GelMA2 hydrogels were dried at −20 °C for 1 day and then in a lyophilizer for 1 day, allowing its porous structure to be examined by SEM. Dried specimens were coated with gold/palladium for 120 seconds using a spray coating machine (SC7620, Quorum, Laughton, East Sussex, UK). Histogram graphs from SEM results of hydrogels and nanofiber were drawn by using an imaging software (Olympus Analysıs, USA). All data is expressed as mean ± standard deviation (n = 3).

2.2.3.3. Mechanical properties

The mechanical properties of GelMA1, GelMA2, GelMA1@PVP and GelMA2@PVP hydrogels were detected with a mechanical testing machine (EZ-LX, Shimadzu, Kyoto, Japan). For each group, three different samples were tested. The compression test was applied to hydrogels. Cylindrical hydrogels 4 mm in height and 3 mm in diameter were prepared for compression testing was calculated using a digital micrometre (Mitutoyo MTI Corp., USA). The compression tests were carried out at a rate of 1 mm per minute up to a maximum of 50% strain.

2.2.3.4. Swelling behaviours

Swelling measurements were performed to determine the water uptake capacity of the hydrogels. For the swelling tests, phosphate buffered saline (PBS) at pH 7.4 was used. During these tests, the initial weights of the hydrogels and nanofibers were of equal weight were recorded. The samples were then transferred to Eppendorf tubes containing 2 ml PBS and kept at 37 °C in a thermal shaker (Microtest). After a certain period of time, the samples were removed from the excess water and the wet weight of the samples was measured [37]. Swelling was measured using equation (2).

$$Swelling\ ratio\ (\%) = \frac{Ww - W_0}{W_0} \times 100\% \quad (2)$$

2.2.4. Cytocompatibility

In vitro cytotoxicity for NIH/3T3 mouse fibroblast cells (ATCC; CRL1658) was evaluated by XTT cell viability assay. To determine cell viability, direct cell culture were used in a 96-well plate. NIH/3T3 mouse fibroblast cells (ATCC; CRL1658) were cultured as described in previous [38]. Briefly, they were cultured in DMEM/F-12 containing 10% FBS and 1% penicillin–streptomycin in a 37 °C, 5% CO_2 incubator. The medium, which was examined under an inverted microscope (BEL, INV100), was changed approximately every 3 days, and when nearly 80% of the cell layer was formed, it was separated from the medium with trypsin/EDTA solution. Prior to cell culture, the hydrogels were sterilized with UV light for 1 h. For cell culture, 2×10^4 cells were planted in a 96 well plate and kept at 37 °C and 5% CO_2 incubator for 1 day. GelMA1 and GelMA2 hydrogels were added and incubated for 1, 3 and 7 days. Cells in the well without hydrogel were used as a control and the experiment was performed in at least three replicates. After the incubation at the end of each day, 100 μl of XTT powder and XTT solution containing PMS in medium was added to each well. Cells were incubated for 4 h in a dark environment, and absorbance values were measured at 450 nm using a microplate reader (Lab-Line Instr., Inc.). Percentage of cell viability was calculated for cell culture method [39]. Cell viability (%) was measured using equation (3).

$$Cell\ viability\ (\%) = \frac{OD\ treatment}{OD\ Control} \times 100\% \quad (3)$$

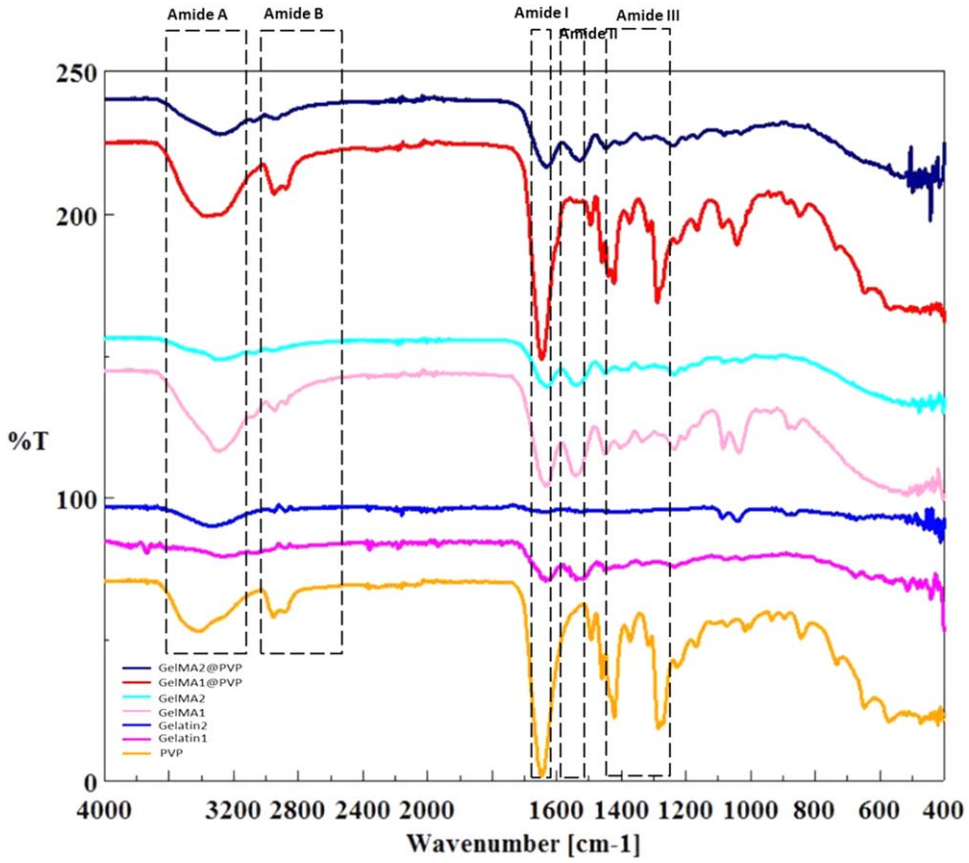

Figure 1. FTIR spectra showing the Amide A, Amide B, Amide I, Amide II, and Amide III regions: PVP, Gelatin1, Gelatin2, GelMA1, GelMA2, GelMA1@PVP and GelMA2@PVP.

2.2.5. Statistical analysis

Statistical analysis was performed using GraphPad Prism 9 software with one-way ANOVA test and two-way ANOVA test as appropriate. Statistical analysis for mechanical and physical analyses was performed using Tukey's multiple comparison test with one-way ANOVA test.

Statistical analysis on cytocompatibility data was analyzed by two-way ANOVA with Tukey's multiple comparison test. It was performed with. Appropriate symbols are used to indicate the p value in the graphs shown; ns = $p > 0.05$, * = $p \leqslant 0.05$, ** = $p \leqslant 0.01$, *** = $p \leqslant 0.001$, **** = $p \leqslant 0.0001$.

3. Results and discussion

3.1. Chemical groups

FTIR was used to determine the chemical structure of PVP, gelatins, GelMAs, as shown in figure 1. FTIR measurement was performed to identify the possible biomolecules, bonds responsible for the structural and functional stabilization of the biomaterials used in the scaffold production. Polypeptide and protein repeats units, consisting of nine characteristic IR bands named amide A, B, and I-VII, represent different vibration points [40]. The amide A band around 3500 cm^{-1} and amide B around 3100 cm^{-1} originate from a Fermi resonance between the first overtone of amide II and the N-H stretching vibration. The amide I band between 1600 and 1700 cm^{-1} is mainly associated with the C=O stretching vibration. Conformationally sensitive amide II band around 1500 cm^{-1} results from the N-H bending vibration and from the C-N stretching vibration. Amide III band between 1400 and 1250 cm^{-1} is associated with complex bands . The polypeptide conformation is directly related to the amide I, II and III band regions of the spectrum.

FTIR spectrum of PVP: the band at 1644 cm^{-1} is C=O associated with stretching groups (Amide I), 1421 cm^{-1} C–H deformations and 1286 cm^{-1} bands is C–N stretching (Amide III), 2951 cm^{-1} the band at can be attributed to C–H stretching (Amide B), and the band at 3419 cm^{-1} can be attributed to associated with O–H stretching (Amide A) [41, 42]. In the GelMA spectrum, the absorption band at 1630 cm^{-1} is associated with the C=O stretching groups (Amide I) and the peak at 1535 cm^{-1} is associated with the N-H bending groups (Amide II). The amide II band in gelatin shifted to 1535 cm^{-1} in GelMA [43]. The absorption band at 1242 cm^{-1} is C–N

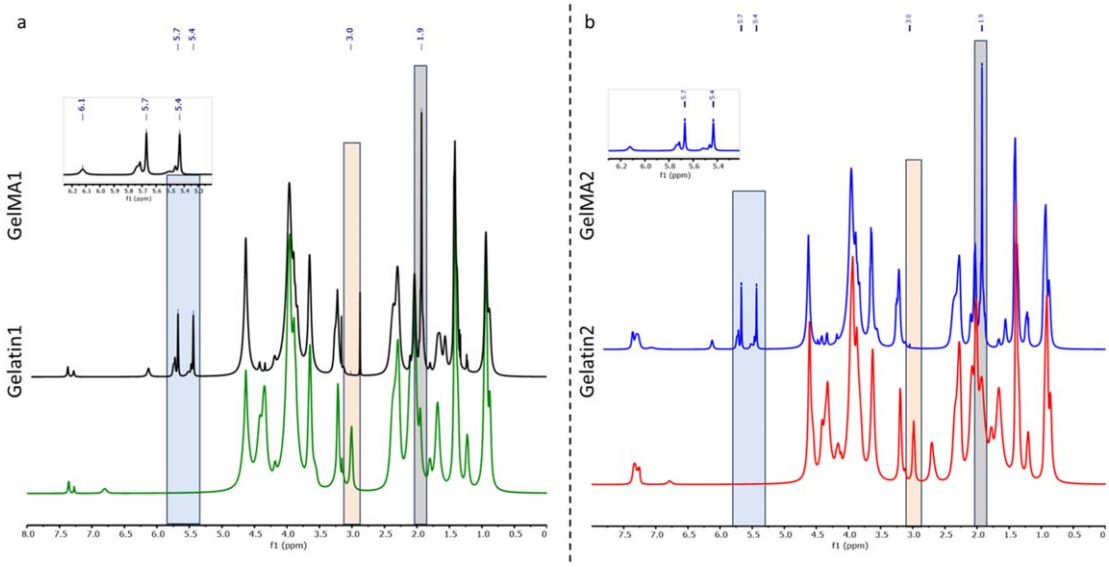

Figure 2. ^{1}H-NMR spectra of gelatin and GelMA samples: (a) Gelatin1 and GelMA1, (b) Gelatin2 and GelMA2.

stretching and N–H bending (Amide III). In addition, the peak at 3278 cm^{-1} is associated with the presence of peptide bonds O-H and N-H functional groups (Amide A) [43, 44]. There was no difference between the characteristic bands of GelMA1 and GelMA2. Due to the overlapping of the characteristic bands of PVP and GelMA and the very low amount of particles in the GelMA@PVP hydrogels, we can say that slight shifts in the peaks of the GelMA@PVP hydrogels compared to GelMA indicate the presence of PVP. There was no difference between the characteristic bands of GelMA1 and GelMA2.

^{1}H NMR analysis was performed to confirm the successful substitution of gelatin with methacryloyl groups (figure 2). ^{1}H NMR analyses were performed using MestReNova software (v12.0.2). Automated phase and baseline verification was performed prior to analysis, and the chemical shift was corrected by reference to the 4.79 ppm value of the deuterium oxide solvent peak. ^{1}H-NMR analysis confirmed that the functional amino groups in the lysine amino acid in the structure of gelatin were methacrylated. In the spectrum of methacrylated gelatin, peaks resulting from methacrylation are observed at chemical shifts of 5.4 and 5.7 ppm. In addition, the peak observed at the chemical shift value of 6.1 ppm shows that methacrylation also occurs through hydroxyl groups. As a result of methacrylation, the effect of methyl protons associated with methacrylation is also seen at the chemical shift value of 1.9 ppm. The peak at 3.06 and 2.90 ppm shift values belonging to lysine methylene (2H) in gelatin disappeared as a result of methacrylation [45]. Phenylalanine signals (7.41–7.25) were taken as reference for DS calculation. Since the lysine methylene field value was obtained as 0 in GelMA, the DM value was calculated as 100% for both samples.

According to the TNBS method results, the amino groups of Gelatin1 were methacrylated at a rate of 88.8 $\pm$ 6.3%, whereas those of Gelatin2 reacted at a rate of 90.4 $\pm$ 2.9%. The lower DS value obtained from the TNBS results has also been observed in other studies. This discrepancy is attributed to the fact that the free lysine groups remaining after methacrylation cannot be effectively determined due to the water suppression effect in the ^{1}H-NMR spectrum signal [36].

3.1.1. Morphology of Hydrogels

The morphology of the hydrogels was examined by SEM and the micrographs are shown in figure 3. In hydrogels, pore size is responsible for many important parameters such as influencing higher cellular activities including degradation profile, drug transport, cell penetration and differentiation [46]. The SEM image of lyophilized GelMA1 and GelMA2 hydrogels showed an irregular porous structure, consistent with the literature, and the average pore diameter was measured to be 6.0 $\pm$ 1.7 μm and 14.16 $\pm$ 4.6 μm. Based on this pore size, it can be assumed that the cells have an opening that can facilitate nutrient-oxygen uptake and infiltration [47, 48]. Based on this pore size, it can be assumed that the cells have an opening that can facilitate nutrient-oxygen uptake and infiltration [47, 48]. In the morphology of PVP particles, the particle diameters were measured to be 689 $\pm$ 130 nm. When the particles appear spherical, it can be assumed that the solvent has completely evaporated [25]. These particle sizes may have the advantage of protecting components (such as drugs) loaded into them [49].

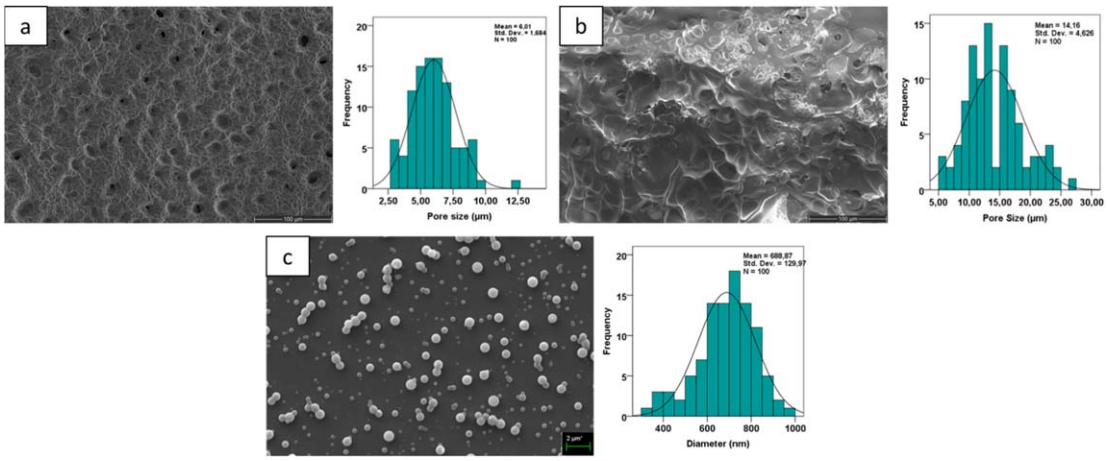

Figure 3. SEM images of hydrogels; (a) GelMA1, (b) GelMA2 and (c) PVP particles.

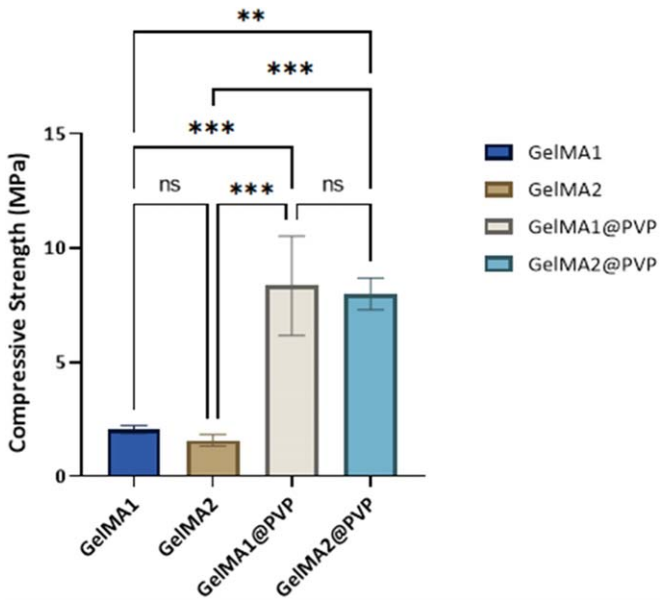

Figure 4. Compressive properties of GelMA1, GelMA2, GelMA1@PVP and GelMA2@PVP hydrogels.

3.2. Mechanical properties

The structure of hydrogels affects their mechanical and swelling properties. Additionally, the mechanical properties of hydrogels play a crucial role in regulating the interactions between cells and the extracellular matrix, as mass flow through the matrix is affected. Moreover, the phenotype and genotype of the cells are controlled by the mechanical properties of the hydrogels [47]. The compressive strength curves showed that the GelMA1 hydrogels had the highest compressive strength of 2.045 MPa, which was higher than that of the GelMA2 hydrogels of 1.564 MPa. The compressive strength of PVP-coated GelMA was measured to be 8.337 MPa for GelMA1@PVP and 7.972 MPa for GelMA2@PVP (figure 4). Although there was no major difference between the hydrogels of two different brands prepared at the same concentrations and UV exposure times, it was observed that the compressive strength of GelMA1 and GelMA1@PVP hydrogels was higher than that of GelMA2 and GelMA2@PVP hydrogels, which can be interpreted as having more functional cross-links [50]. On the other hand, the increase in compressive strength of the hydrogel may indicate that it can withstand external pressure when implanted in a defective area [51]. In addition, PVP may increase mechanical strength by binding to GelMA hydrogels and acting as a crosslinker. In addition, the fact that the pore size of the GelMA2 group is larger than that of the GelMA1 group may reveal the correct proportion of the SEM analysis of the difference in mechanical strength and physical behavior. Statistical analysis was performed using Graphad Prism

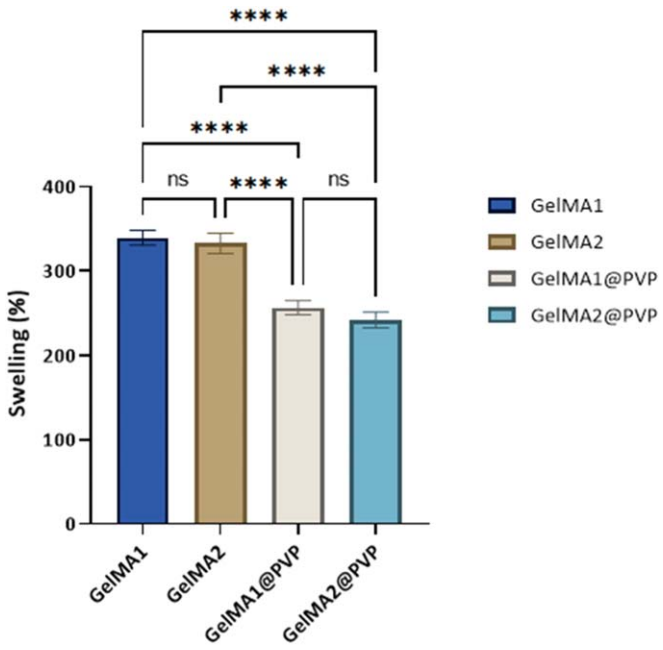

Figure 5. Swelling behavior of GelMA1, GelMA2, GelMA1@PVP and GelMA2@PVP hydrogels.

9 software. Data were analyzed by ANOVA with one-way ANOVA test. Statistical difference is indicated by *** $p < 0.001$. Error bars represent standard deviations (SDs) of measurements made on at least three samples.

3.3. Swelling behaviours

The swelling capacity of the hydrogel is critical for the strength of the scaffold, load release during the healing period, and cell attachment [52]. To investigate their swelling behavior, mass changes over time were measured when GelMA1 and GelMA2 hydrogels and GelMA2@PVP were incubated in PBS solution for 120 min at 37 °C. The swelling behavior of the hydrogels (figure 5) increased significantly within the first 5 min. Swelling equilibrium was reached in 45 min for GelMA1 and GelMA2 hydrogels and in 60 min GelMA1@PVP and GelMA2@PVP hydrogels. It is seen that the swelling rate of GelMA1 (~339%) and GelMA2 (~332%) are upper than that of GelMA1@PVP (~256%) GelMA2@PVP (~242%). Variation in the degree of methacrylation, amount of photoinitiator, pore size and type of solvent of the GelMA hydrogel affects the swelling property. Considering the morphology analysis, the fact that the pore size of the GelMA2 hydrogel group is higher than that of the GelMA1 hydrogel group is not reflected in the swelling properties. Because there is no significant difference between GelMA1 and GelMA2 in terms of swelling behavior. Also, the slight difference between the two GelMA hydrogels (Sigma and Halvet) can be attributed to the change in the number of hydrophilic groups in the hydrogels [48, 53]. It can be thought that coating GelMA@PVP with particles reduced the water absorption capacity of the hydrogel [52]. Significant differences in the mass swelling ratio may be due to the fact that the hydrogels are coated with PVP and contain fewer hydrophobic amino acids, making those with a higher swelling ratio more hydrophilic than those with a lower swelling ratio [54]. Statistical analysis was performed using Graphad Prism 9 software. Data were analyzed by ANOVA with one-way ANOVA test. Statistical difference is indicated by **** $p < 0.0001$. Error bars represent standard deviations (SDs) of measurements made on at least three samples.

3.4. Cytocompatibility

The XTT assay was performed on hydrogels cultured with NIH/3T3 mouse fibroblast cells. The ability of GelMA1 and GelMA2 hydrogels to support cell viability was confirmed. In XTT analysis, all hydrogels showed biocompatibility. According to the 7-day results, the cell viability in GelMA1 is 139%. Cell viability in GelMA2 is 133%. At the end of day 7, the percentage cell viability for the GelMA1 and GelMA2 hydrogels compared to the control group (compared to the NIH/3T3 cell control as 100%) was significant (****$p<0.0001$). In addition, no significant difference was found between GelMA1 and GelMA2 at the end of day 7. Data are expressed as mean ± SD for all cell culture methods and are statistically significant compared to control. Statistical analysis was performed using GraphPad Prism 9 software. Data were analyzed by ANOVA with Tukey's multiple comparison test (figure 6).

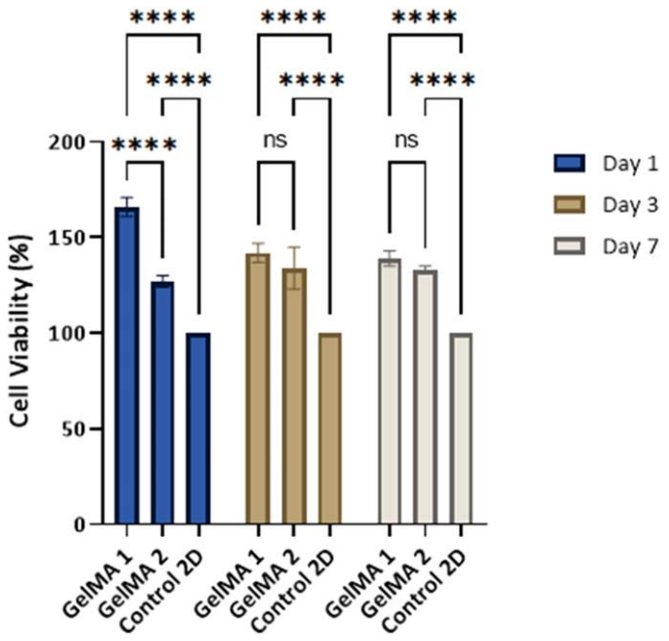

Figure 6. Percent cell viability in GelMA1 and GelMA2 hydrogels.

4. Conclusions

To summarize, two different GelMA syntheses were successfully prepared from type B gelatin of two different products. There was no significant difference between the mechanical, physical and biological behaviors of GelMA hydrogels from two different products under the same methacrylation conditions and UV exposure times, except for differences in pore size. Differences in pore size also did not show significant differences in other behaviors.

We believe that their use in biomedical applications will yield successful results as the resulting hydrogels show relatively favorable swelling performance, good mechanical properties and cytocompatibility. In light of the results obtained, show that coating GelMA hydrogels with PVP has the potential to be used in tissue engineering products integrated with many drug delivery systems in the future.

Acknowledgments

This study was supported by the Turkish Scientific and Technical Research Council (TUBITAK) 1001 Project—TracPatch. The project number is 222M048. Hilal YILMAZ was supported by both YÖK 'Biomedical Technology and Equipment (Design-Manufacturing and Supply)' Doctoral Program YÖK 100/2000. We would like to thank YÖK and TUBITAK for their financial support during this work.

Data availability statement

All data that support the findings of this study are included within the article (and any supplementary files).

Conflict of interest

The authors declare no conflict of interest.

ORCID iDs

Hilal Yilmaz https://orcid.org/0000-0003-3326-4873
Arsalan Ahmed https://orcid.org/0000-0003-4099-0101
Cem Bulent Ustundag https://orcid.org/0000-0002-4439-0878

References

[1] Yue K *et al* 2015 Synthesis, properties, and biomedical applications of gelatin methacryloyl (GelMA) hydrogels *Biomaterials* **73** 254–71
[2] Peyret C *et al* 2023 Gelatin methacryloyl (GelMA) hydrogel scaffolds: predicting physical properties using an experimental design approach *Int. J. Mol. Sci.* **24** 13359
[3] Lv B *et al* 2023 Recent advances in GelMA hydrogel transplantation for musculoskeletal disorders and related disease treatment *Theranostics* **13** 2015
[4] Sun M *et al* 2018 Synthesis and properties of gelatin methacryloyl (GelMA) hydrogels and their recent applications in load-bearing tissue *Polymers* **10** 1290
[5] Van Den Bulcke A I *et al* 2000 Structural and rheological properties of methacrylamide modified gelatin hydrogels *Biomacromolecules* **1** 31–8
[6] Lee B H *et al* 2016 Synthesis and characterization of types A and B gelatin methacryloyl for bioink applications *Materials* **9** 797
[7] Chen Y *et al* 2022 Comparison of globular albumin methacryloyl and random-coil gelatin methacryloyl: preparation, hydrogel properties, cell behaviors, and mineralization *Int. J. Biol. Macromol.* **204** 692–708
[8] Young A T, White O C and Daniele M A 2020 Rheological properties of coordinated physical gelation and chemical crosslinking in gelatin methacryloyl (GelMA) hydrogels *Macromol. Biosci.* **20** 2000183
[9] Tümerkan E T A 2021 Sustainable utilization of gelatin from animal-based Agri–food waste for the food industry and pharmacology *Valorization of Agri-Food Wastes and By-Products* (*Recent Trends, Innovations and Sustainability Challenges*) (Academic) ch 21 425–42
[10] Suvarnapathaki S *et al* 2019 Synthesis and characterization of photocrosslinkable hydrogels from bovine skin gelatin *RSC Adv.* **9** 13016–25
[11] Shirahama H *et al* 2016 Precise tuning of facile one-pot gelatin methacryloyl (GelMA) synthesis *Sci. Rep.* **6** 31036
[12] Chen S *et al* 2023 Structure and properties of gelatin methacryloyl (GelMA) synthesized in different reaction systems *Biomacromolecules* **24** 2928–41
[13] Gao C *et al* 2021 Hydrogel composite scaffolds with an attenuated immunogenicity component for bone tissue engineering applications *J. Mater. Chem.* B **9** 2033–41
[14] Li L, Scheiger J M and Levkin P A 2019 Design and applications of photoresponsive hydrogels *Adv. Mater.* **31** 1807333
[15] Peng K *et al* 2022 Light manipulation for fabrication of hydrogels and their biological applications *Acta Biomater.* **137** 20–43
[16] Tomatsu I, Peng K and Kros A 2011 Photoresponsive hydrogels for biomedical applications *Adv. Drug Delivery Rev.* **63** 1257–66
[17] Wang Z *et al* 2017 Comparative study of gelatin methacrylate hydrogels from different sources for biofabrication applications *Biofabrication* **9** 044101
[18] Gaglio C G *et al* 2024 GelMA synthesis and sources comparison for 3D multimaterial bioprinting *Front. Bioeng. Biotechnol.* **12** 1383010
[19] Choukaife H, Doolaanea A A and Alfatama M 2020 Alginate nanoformulation: Influence of process and selected variables *Pharmaceuticals* **13** 335
[20] Zamani M, Prabhakaran M P and Ramakrishna S 2013 *Advances in drug delivery* via *electrospun and electrosprayed nanomaterials Int. J. Nanomed.* **8** 2997–3017
[21] Alfatama M, Shahzad Y and Choukaife H 2024 Recent advances of electrospray technique for multiparticulate preparation: drug delivery applications *Adv. Colloid Interface Sci.* **325** 103098
[22] Ding D and Zhu Q 2018 Recent advances of PLGA micro/nanoparticles for the delivery of biomacromolecular therapeutics *Materials Science and Engineering:* C **92** 1041–60
[23] Cui L *et al* 2014 Electrosprayed core–shell nanoparticles of PVP and shellac for furnishing biphasic controlled release of ferulic acid *Colloid. Polym. Sci.* **292** 2089–96
[24] Koczkur K M *et al* 2015 Polyvinylpyrrolidone (PVP) in nanoparticle synthesis *Dalton Trans.* **44** 17883–905
[25] Narváez-Muñoz C, Ryzhakov P and Pons-Prats J 2021 *Determination of the operational parameters for the manufacturing of spherical PVP particles* via *electrospray Polymers* **13** 529
[26] Edikresnha D, Sriyanti I and Munir M 2017 Synthesis of Polyvinylpyrrolidone (PVP)-Green tea extract composite nanostructures using electrohydrodynamic spraying technique *IOP Conf. Series: Materials Science and Engineering* (IOP Publishing)
[27] Chhouk K *et al* 2018 *Micronization for enhancement of curcumin dissolution* via *electrospraying technique ChemEngineering* **2** 60
[28] Rezeki Y *et al* 2019 Synthesis of polyvinylpyrrolidone/mangosteen pericarp extract (MPE) fibered particles using electrospray *Journal of Physics: Conf. Series* (IOP Publishing)
[29] Guastaferro M *et al* 2020 Supercritical assisted electrospray/spinning to produce PVP+ quercetin microparticles and microfibers *J. Taiwan Inst. Chem. Eng.* **117** 278–86
[30] Ali R *et al* 2020 Electrospinning/electrospraying coatings for metal microneedles: a design of experiments (DOE) and quality by design (QbD) approach *Eur. J. Pharm. Biopharm.* **156** 20–39
[31] Belyy V *et al* 2021 Water stable colloidal lignin-PVP particles prepared by electrospray *Int. J. Biol. Macromol.* **190** 533–42
[32] Xu L *et al* 2023 Electrosprayed core (cellulose acetate)–shell (polyvinylpyrrolidone) nanoparticles for smart acetaminophen delivery *Pharmaceutics* **15** 2314
[33] Yılmaz H *et al* 2024 Development of bilayer tissue-engineered scaffolds: combination of 3D printing and electrospinning methodologies *Biomed. Mater.* **19** 045029
[34] Aramwit P *et al* 2015 A comparative study of type A and type B gelatin nanoparticles as the controlled release carriers for different model compounds *Mater. Express* **5** 241–8
[35] Tasci M E *et al* 2021 Production, optimization and characterization of polylactic acid microparticles using electrospray with porous structure *Applied Sciences* **11** 5090
[36] Claaßen C *et al* 2018 Quantification of substitution of gelatin methacryloyl: best practice and current pitfalls *Biomacromolecules* **19** 42–52
[37] Wang J, Su S and Qiu J 2017 Biocompatible swelling graphene oxide reinforced double network hydrogels with high toughness and stiffness *New J. Chem.* **41** 3781–9
[38] Koc E *et al* 2023 Methylprednisolone 100 mg tablet formulation with pea protein: experimental approaches over intestinal permeability and cytotoxicity *Drug Dev. Ind. Pharm.* **49** 467–78
[39] Foo J B *et al* 2019 Induction of cell cycle arrest and apoptosis by copper complex Cu (SBCM) 2 towards oestrogen-receptor positive MCF-7 breast cancer cells *RSC Adv.* **9** 18359–70
[40] Das M P *et al* 2017 Extraction and characterization of gelatin: a functional biopolymer *Int. J. Pharm. Pharm. Sci* **9** 239
[41] Mireles L K *et al* 2020 Physicochemical characterization of polyvinyl pyrrolidone: a tale of two polyvinyl pyrrolidones *ACS omega* **5** 30461–7

[42] Safo I et al 2019 The role of polyvinylpyrrolidone (PVP) as a capping and structure-directing agent in the formation of Pt nanocubes *Nanoscale Advances* **1** 3095–106
[43] Jamshidifar E et al 2022 Improvement of in vitro osteogenesis and anti-infection properties by GelMA scaffold containing levofloxacin nanoparticles and strontium microspheres for osteomyelitis *J. Mater. Sci.* **57** 13603–19
[44] Erkus H et al 2023 Innovative transdermal drug delivery system based on amoxicillin-loaded gelatin methacryloyl microneedles obtained by 3D printing *Materialia* **27** 101700
[45] Hu Q et al 2024 Precision engineering of chondrocyte microenvironments: investigating the optimal reaction conditions for type B gelatin methacrylate hydrogel matrix for TC28a2 cells *Journal of Functional Biomaterials* **15** 77
[46] Tang L et al 2023 GelMA hydrogel loaded with extracellular vesicles derived from umbilical cord mesenchymal stem cells for promoting cutaneous diabetic wound healing *ACS omega* **8** 10030–9
[47] Yin H et al 2023 Physical properties and cellular responses of gelatin methacryloyl bulk hydrogels and highly ordered porous hydrogels *Frontiers in Soft Matter* **2** 1101680
[48] Liu T et al 2021 Effect of freezing process on the microstructure of gelatin methacryloyl hydrogels *Front. Bioeng. Biotechnol.* **9** 810155
[49] Sen Gupta A 2016 Role of particle size, shape, and stiffness in design of intravascular drug delivery systems: insights from computations, experiments, and nature *Wiley Interdiscip. Rev. Nanomed. Nanobiotechnol.* **8** 255–70
[50] Baykara D et al 2023 Fabrication and optimization of 3D printed gelatin methacryloyl microneedle arrays based on vat photopolymerization *Front. Bioeng. Biotechnol.* **11** 1157541
[51] Choi J-B et al 2021 Fabrication and characterization of biodegradable gelatin methacrylate/biphasic calcium phosphate composite hydrogel for bone tissue engineering *Nanomaterials* **11** 617
[52] Shi Y et al 2023 Preparation of a 3D printable high-performance GelMA hydrogel loading with magnetic cobalt ferrite nanoparticles *Front. Bioeng. Biotechnol.* **11** 1132192
[53] Rahali K et al 2017 Synthesis and characterization of nanofunctionalized gelatin methacrylate hydrogels *Int. J. Mol. Sci.* **18** 2675
[54] Elkhoury K et al 2021 *Synthesis and characterization of C2C12-laden gelatin methacryloyl (GelMA) from marine and mammalian sources Int. J. Biol. Macromol.* **183** 918–26